

Bursts in Material of Low Atomic Number*

F. E. DRIGGERS†

Randall Laboratory of Physics, University of Michigan, Ann Arbor, Michigan

(Received April 24, 1952)

A large ionization chamber has been used to obtain an integral burst size-frequency distribution by amplifying and recording the electron pulses produced by bursts. A comparison of the integrated burst rate from the upper hemisphere with that produced by primaries with a small zenith angle permitted an estimate of the burst rate resulting from interactions of the N component. Calculations were made of the expected burst distributions arising from the electromagnetic interactions (bremsstrahlung, knock-on, and direct pair production) of spin 0 and spin $\frac{1}{2}$ μ -mesons. About $\frac{1}{3}$ of the bursts observed under 400 g cm^{-2} of sand-lime brick and concrete at sea level were attributed to interactions of the N component. The remaining burst rate agreed with the rate calculated for spin $\frac{1}{2}$ to within the estimated uncertainty of the comparison—about 20 percent. Lack of quantitative information concerning the nuclear interactions of μ -mesons prevents an estimation of the actual electromagnetic cross sections. The expected Z dependence of μ -meson bursts was roughly confirmed by a comparison with results obtained elsewhere under material of higher Z .

1. INTRODUCTION

ALTHOUGH many experiments on bursts have been performed under various conditions, only those of Schein and Gill¹ under lead and of Lapp² under iron have been suitable for comparison with the only available analysis of the burst rate to be expected from the bremsstrahlung and knock-on interactions of μ -mesons. This analysis was performed by Christy and Kusaka³ for assumed values of the spin of 0, $\frac{1}{2}$, and 1. Comparison with experimental results is limited by the fact that this analysis was specifically designed for a spherical ionization chamber. A comparison between these experiments and the calculations have evidenced a definite disagreement with the expected burst rate for spin 1 μ -mesons but have failed to distinguish conclusively between the possibilities of spin 0 and spin $\frac{1}{2}$. Part of the reason for this failure is connected with the atomic number of the material surrounding the chamber.

The cross section for bremsstrahlung, which is the process making the largest contribution to the number of bursts of very large size, was derived by Heitler⁴ using a Born approximation which was valid only if $2\pi Ze^2/\hbar v_0 \ll 1$, where Z is the atomic number of the material concerned and v_0 is the velocity of the incoming charged particle. Even for $v_0 \sim c$, this quantity has a value of 0.6 for lead, making the use of the approximation rather doubtful. For iron, this quantity is 0.2 and the approximation is considerably better.

Furthermore, cascade shower theory plays an important role in the analysis of this theoretical burst rate, and the approximations used are valid for high

energy electrons and photons but are of doubtful validity for the low energy range. Since the critical energy β , which is roughly proportional to Z^{-1} , is in a sense a measure of the lowest energy an electron can have and still play a significant role in the further development of a shower, these approximations, which are very poor for lead, become better as the atomic number of the material around the chamber is decreased.

In order to permit a more valid theoretical calculation for comparison with experimental results, the present experiment *A* was designed to measure the burst rate under considerable thicknesses of material of low atomic number. In addition, the use of a material of low atomic number permits a more sensitive test of the Z dependence of these bursts than has been possible previously.

The burst rate observed in experiment *A* was somewhat larger than the calculated burst rate due to μ -meson interactions for this geometry. Experiment *B* was designed and performed to obtain information concerning the angular dependence and the absorption in lead of the primaries responsible for these excess bursts. The design was predicated on a tentative attribution of these excess bursts to interactions of the N component.

2. EXPERIMENTAL APPARATUS

Since the equipment was designed for the purpose of measuring the rate of bursts due to the high energy interactions of μ -mesons, provision had to be made to eliminate or identify, in some way, other types of bursts. A large amount of ionization may be produced in the ionization chamber by two distinct classes of events; that is, emission of an α -particle by an atom on or near the surface of the inner walls of the chamber plates or by one of several types of events associated with cosmic radiation. To minimize the useless recording of events of the first type, it was required that ionization in the chamber be accompanied by the discharge of one or more of the Geiger tubes in the coincidence tray.

The ionizing events associated with cosmic rays may be further divided into soft showers (mainly produced

* The research was aided by a grant to the cosmic-ray program of the University of Michigan from the joint program of the AEC and ONR and by a fellowship of 18 months duration administered by the AEC.

† Now with E. I. duPont de Nemours and Company, Argonne National Laboratory, Chicago, Illinois.

¹ M. Schein and P. S. Gill, *Revs. Modern Phys.* **11**, 267 (1939).

² R. E. Lapp, *Phys. Rev.* **69**, 312 (1946).

³ R. F. Christy and S. Kusaka, *Phys. Rev.* **59**, 414 (1941).

⁴ W. Heitler, *The Quantum Theory of Radiation* (Oxford University Press, London, 1936).

by μ -meson interactions in the material around the chamber) and nuclear events (produced by the few protons and π -mesons in the hard component at sea level). To some extent, it is possible to distinguish between these two types by the shape of the voltage pulse produced on the collecting wires. Some of the soft showers recorded may be expected to result when the core of an Auger shower strikes in the vicinity of the chamber. An auxiliary record was made of those soft-shower-like chamber pulses which were accompanied by the discharge of one or both of the Geiger tubes in the air-shower tray, which was located in the open a few feet from the chamber.

The equipment used in this experiment is displayed in symbolic form in the block diagram, Fig. 1, which is largely self-explanatory.

The chamber was constructed in the form of a rectangular parallelepiped. The top and bottom of the chamber are 1-inch thick Duralumin plates and the four sides are $\frac{5}{16}$ -inch steel plates. The steel plates are 8.0 inches high and were welded together to form a rectangular area of dimension 24 inches by 92 inches. These plates were grounded and served as the cathode. As anodes, 6 wires were suspended halfway between the Duralumin plates and parallel to the long axis of the chamber. The volume controlled by each of the 4 collecting wires (the pulses induced on the two outer wires were not measured) was 4 inches wide, 8 inches high, and 86 inches long. These sensitive volumes were not bounded by the steel plates, protection being afforded either by dummy wires or by guard cylinders around the wires. The chamber was filled with argon at a pressure of 1.40 atmospheres. The argon contained 0.1 percent of unspecified impurities.

Polonium α -particle sources were used for the purpose of calibrating the chamber. The sources were made by plating polonium onto the end of a rod which could be inserted into and withdrawn from the chamber using an O-ring sealing device. For normal chamber operation, the source was withdrawn into a recess outside of the Duralumin plate. For calibration, the source could be moved from the inner surface of the Duralumin to a point 4 inches inside the plate.

The chamber was operated as an electron pulse chamber using a "delay line clipping" method of low frequency rejection.^{5,6} The preamplifiers and amplifier *I* in the block diagram follow the wiring diagram identified in Elmore and Sands⁷ as a Model 100 pulse amplifier, amplifier *I* being only the first of the two negative feedback loops in the main amplifier. The synchroscope follows the design of Fitch and Titterton.⁸ These amplifiers are stable and linear and the distortion in-

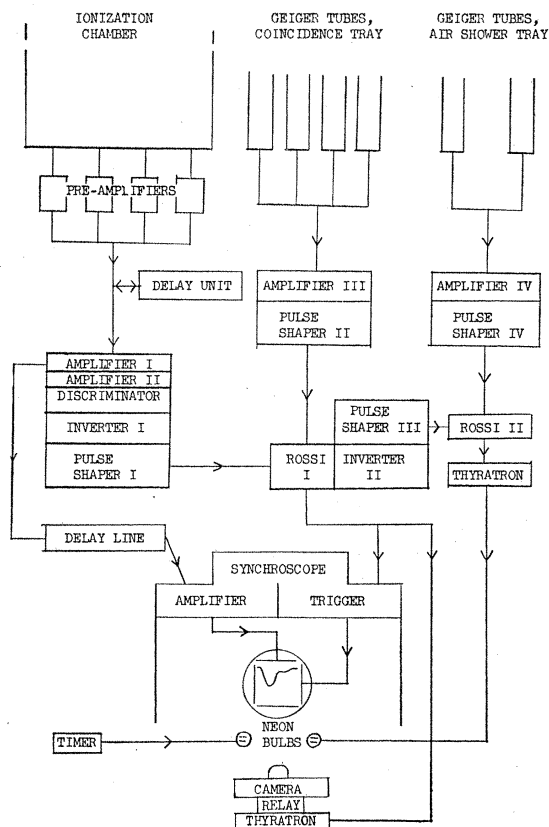


FIG. 1. Block diagram of equipment and electronics.

duced in the pulse is small enough so that significant differences in pulse shapes are not destroyed.

The advantage in using 4 preamplifiers lies in increasing the signal to noise ratio. Most of the input capacity C to the grid of a preamplifier is inside the chamber. For a charge Q induced on one wire, the voltage pulse is $\sim Q/C$. If the noise at the grid of the first tube is N , the signal to noise ratio out of the preamplifier is $\sim Q/CN$ and after combining the output of the four preamplifiers, it is $Q/4^{\frac{1}{2}}CN$, since the noise outputs are random and incoherent. On the other hand, if the four collecting wires are joined before the grid of the first tube, the capacity is nearly $4C$, the signal is $Q/4C$ and the signal to noise ratio out of the preamplifier is $Q/4CN$. A gain of two in this factor is thus obtained.

3. CHAMBER ENVIRONMENT

The experiments were performed in the second basement of Randall Laboratory. Surrounding the room, there is approximately 4 feet of brick, earth, and concrete. The chamber was placed several inches above the concrete floor, which had only sand underneath. The chamber itself was surrounded, except underneath, by a minimum of 116 cm of commercial sand-lime brick as illustrated in Fig. 2. The ends of the chamber were surrounded in a similar fashion with the exception of a

⁵ B. Rossi and H. H. Staub, *Ionization Chamber and Counters* (McGraw-Hill Book Company, Inc., New York, 1949).

⁶ Bridge, Hazen, Rossi, and Williams, *Phys. Rev.* **74**, 1083 (1948).

⁷ W. C. Elmore and M. Sands, *Electronics* (McGraw-Hill Book Company, Inc., New York, 1949).

⁸ V. L. Fitch and E. W. Titterton, *Rev. Sci. Instr.* **18**, 821 (1947).

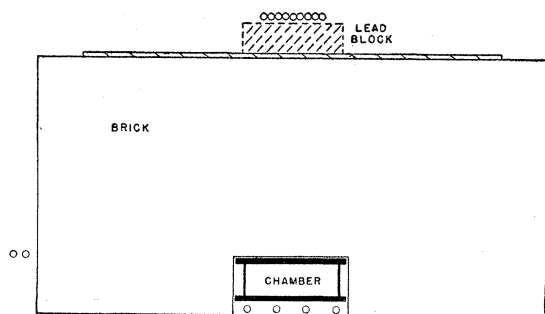


FIG. 2. Cross section of the chamber and environment. The circles under the chamber represent the Geiger tube coincidence tray in experiment A, during which the lead block was not in place. This tray was augmented and moved to the position indicated on top of the brick pile for experiment B. Part of this experiment was performed with the lead block in place and part without. The air-shower tray is represented by the two circles at the left outside the brick pile.

tunnel which led through the brick pile and was the height and width of the chamber. This permitted access to the preamplifiers, Geiger tubes, and the connecting leads. In addition, a 1-inch layer of lead covered most of the top of the brick pile.

In terms of the radiation length,

$$X_0 = [4\alpha(N/A)r_0^2Z(Z+1)\log 183Z^{-1}]^{-1},$$

where $\alpha = 1/137$, $r_0 = 2.82 \times 10^{-13}$, $N = 6.02 \times 10^{23}$, and Z and A are the atomic number and weight, respectively, of the material, the chamber was shielded by ~ 9 radiation lengths in the building, 9.2 radiation lengths in the pile of brick, and, for some distance around the vertical, by 5 radiation lengths of lead. In terms of mass per unit area, a measure which is appropriate for the elimination of the N component, the building contained ~ 200 g-cm $^{-2}$, the lead contained 30 g-cm $^{-2}$, and the brick pile contributed 180 g-cm $^{-2}$.

The critical energy β for the material was obtained from the Bloch formula for collision energy loss⁹ by setting $-(dE/dx) = \beta/X_0$ and by solving the resulting transcendental equation by successive approximations. I_0 in this equation was taken to have the value 11.5 ev in accordance with the measurements of Wilson.¹⁰ The values of these shower theory parameters which are appropriate for the present arrangement will lie between those for brick (0.90 SiO $_2$, 0.10 CaO) and for Duralumin (0.96 Al, 0.04 Cu) but will be much closer to the values for brick since there is only $\frac{1}{4}$ radiation length of Duralumin between the brick and the sensitive volume of the chamber. For brick and Duralumin, X_0 in g cm $^{-2}$ is 26.5 and 23.6, and β in Mev is 55.7 and 47.1, respectively. For the brick-Duralumin combination, values of $X_0 = 26$ g cm $^{-2}$ and $\beta = 54$ Mev were used.

In experiment A, the coincidence tray of Geiger tubes was placed immediately under the chamber. This arrangement insured that less than 0.1 percent of the

bursts from any part of the upper hemisphere were missed because of the coincidence requirement. The smallest burst recorded contained about 35 particles capable of penetrating the bottom Duralumin plate. In experiment B, the coincidence tray was placed 7 inches above the top of the brick pile in such a position that the center of the tray was above the center of the ion chamber and the long axes of the tray and the chamber were parallel. The coincidence tray in the latter case consisted of 9 closely packed Geiger tubes giving a sensitive tray area of 18 inches by 88 inches. For bursts produced in the brick, the burst-producing particle triggered the coincidence tray. Part of the data in experiment B was gathered with air between the tray and the top of the brick pile and part with an additional 6 inches of lead filling this gap.

4. ELECTRON ATTACHMENT

An expression for the voltage pulse, V_p , produced on a central wire by the collection of the ions in a burst was developed in reference 5. This was

$$V_p = -(e/U_0C) \sum_1^N (U_0 - U_i),$$

where U_0 is the potential of the central wire with respect to the grounded chamber shell, U_i is the potential at the point of formation of one of the N ion pairs in the burst, and e is the electronic charge. It was developed under the assumption of negligible electron attachment. Electron attachment is the process in which an electron collides with a neutral molecule and forms a negative ion (O $_2$ and H $_2$ O are the two most common possibilities). Since the drift of ions is negligible during the collection time of an electron pulse chamber, the electron is essentially lost in this process and V_p is correspondingly smaller.

One customary criterion for freedom from electron attachment is the demonstration that, for a calibration source flush with the wall of the chamber, V_p does not continue to increase as U_0 is increased beyond a certain

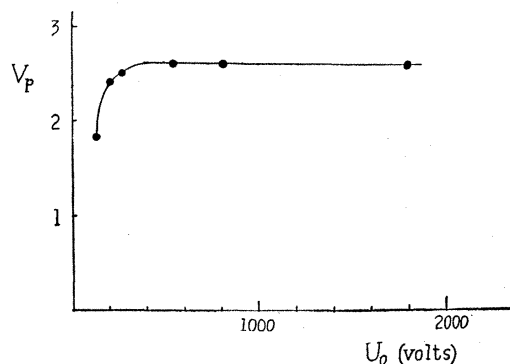


FIG. 3. Maximum voltage pulse V_p in arbitrary units, produced by an α -particle source flush with the chamber walls as a function of the potential difference across the chamber, U_0 , in volts.

⁹ F. Bloch, Z. Physik **81**, 363 (1933).

¹⁰ R. R. Wilson, Phys. Rev. **60**, 749 (1941).

saturation voltage. The experimental values of V_p for a source flush with the chamber wall and directly under a collecting wire are plotted in Fig. 3 in arbitrary units as a function of the potential U_0 of the wire. An operating potential of $U_0=800$ volts was chosen on the basis of these results.

To check the basic criterion, a further series of measurements was made in which U_0 was maintained at 800 volts and the distance from the source to the collecting wire was varied from 4 inches to $\frac{1}{2}$ inch. An example of the results is plotted in Fig. 4. Since, in the absence of electron attachment, $\sum[U_0-U_i(r)]$, and thus V_p , is a constantly decreasing function of r , the experimental points (\odot) indicate that some attachment does exist. The saturation evidenced in Fig. 3 indicates either that w^- , the electron drift velocity, is almost independent of E^- , the field strength, or that the probability of attachment per collision rises for increasing w^- in such a way as to compensate for the decrease in the number of collisions due to the decrease in the collection time.

It is possible to make a rough estimate of the collection time by measuring the corresponding distance on the oscilloscope photograph. The initial slope of the calibration pulses is so small for $r=4$ inches that it is difficult to determine the point at which the pulse started. Within the limits set by this difficulty, the collection time for this value of r was found to be independent of U_0 for the range $400 \text{ volts} < U_0 < 1800 \text{ volts}$. The field strengths at the Duralumin plate as well as throughout the chamber increased by a factor of 4.5 as U_0 was increased. We thus conclude that w^- is independent of E^- over this range. Another series of measurements was made in which r was varied holding U_0 fixed. This also had the effect of varying the average field strength for the electrons concerned, since the field strengths increase as the wire is approached. Measurements of this collection time are plotted in Fig. 5 for $U_0=800$ volts. A straight line through the point $r=0$, $t=0$ fits the data rather well, which again indicates

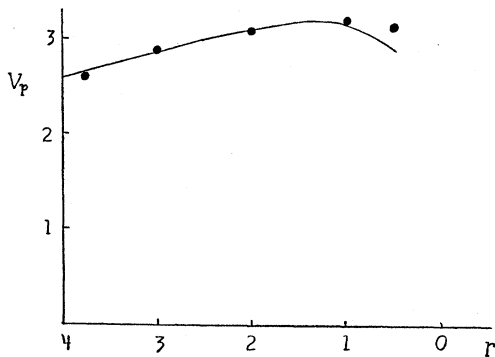


FIG. 4. The solid circles represent the maximum voltage pulse V_p in arbitrary units, produced by an α -particle source r inches from the collecting wire as a function of r for a chamber voltage of 800 volts. The curve is calculated on the basis of a simple model for electron attachment.

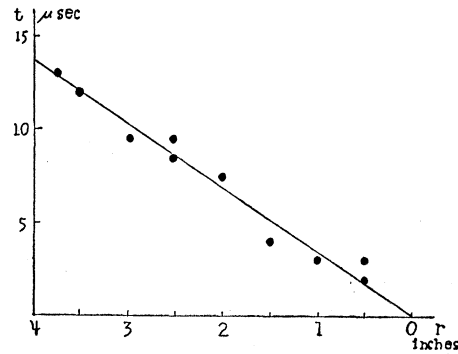


FIG. 5. The collection time t in μ -sec, for the electrons produced by an α -particle source r inches from the collecting wire as a function of r .

that w^- is independent of E^- over a considerable range of field strengths.

In view of this conclusion, a very simple treatment of the effect of electron attachment is possible. We have $dN = kNdr$ and, integrating, $\log N = c + kr$. Thus, if we have originally N_0 electrons produced at a distance r_0 from the wire, the number reaching the wire is $N_w = N_0 e^{-kr_0}$. The contribution to the pulse height of those electrons which reach the wire is $V_p \sim N_0 [U_0 - U(r_0)] e^{-kr_0}$. An electron which is absorbed at a distance r from the wire after being produced at a distance r_0 also makes a contribution proportional to $[U(r) - U(r_0)]$, but since U behaves logarithmically in the neighborhood of the wire, the contribution is usually small and will be neglected.

Before the expression for V_p can be compared to the experimental points, one further consideration must be made. The source is located on a grounded metal rod which projects into the chamber and distorts the potential field. As a first approximation, it was assumed that the effect of the distortion was that the average potential in which the ions from an α -particle are produced is reduced by some constant fraction, b . Thus $V_p \sim N_0 [U_0 - bU(r_0)] e^{-kr_0}$. An attempt to match the experimental points in Fig. 4 by adjusting the parameters b and k in this expression results in a value of b slightly greater than one. In view of the existence of some uncertainty in the experimental results this is not surprising, but physically it is an impossibility. The value of b was therefore taken to be 1.0, and the best fit was then obtained for $k=0.215 \text{ inch}^{-1}$. The curve plotted in Fig. 4 represents the above expression for V_p with these values of the parameters inserted. It should be mentioned that the value of k does not depend very critically on the value of b . If b had been assumed to be 0.8, k would have been 0.19 inch^{-1} . Several typical photographs on which the experimental points were measured are shown in Fig. 6.

A comparison may now be made between the two extreme cases of ionization distribution in the chamber involved in calibrating the chamber by integrating numerically the expression $[U_0 - U(r_0)] e^{-kr_0}$ over the

appropriate volumes in the two cases and normalizing to N_0 original ions. If the same number of ions is distributed uniformly throughout the chamber or, on the other hand, is concentrated near one of the grounded plates of the chamber, the locally ionizing event (calibration type) will produce a pulse which is 4.9 percent lower than the generally ionizing event (burst type).

5. CHAMBER CALIBRATION

If, with the calibration source flush with the wall, the number $N(h)$ of α -particle pulses larger than a size h is plotted as a function of h , a curve similar to Fig. 7 in reference 6 is obtained. The maximum pulse size produced by an α -particle h_α may be taken as the h value obtained by extrapolating the nearly vertical, linear portion of this curve to zero frequency. About 75 percent of the pulses have a size which is not more than 3 percent smaller than h_α , and the number that have a size more than 3 percent larger than h_α is less than 1 percent of the total. It might be anticipated that, out of a group of about ten consecutive pulses, the largest would usually lie within 3 percent of h_α . This was demonstrated to be the case.

Thus the calibration procedure adopted during the experiment was to superimpose on the film, the synchroscope traces of a group of from five to twenty pulses from the calibration source flush with the chamber wall. Such a group is illustrated in Fig. 6, $U_0=800$, $r=4$. A record of five such groups was made in each calibration, and in general, the largest pulse in each of the five groups did not differ from any of the other largest pulses by more than the accuracy of measurement—that is, about 3 percent. Occasionally, one deviant in a group of five was eliminated before h_α was determined as the mean of the largest pulse in each of the groups.

Some of these deviants were recognizable as being the result of the superposition of two α -particle pulses. Other smaller deviations may have been due to noise fluctuations superimposed on some of the pulses.

This procedure was repeated for each of the four collecting wires and signal channels, the measurements were corrected for the results of electron attachment,

and it was required that h_α for the four wires agree to within 5 percent before the related burst results were used. This requirement was imposed to insure that the gains of the four preamplifiers were the same within 5 percent. This was necessary because the outputs of the preamplifiers were mixed together and corrections for differences in gain could not be made. The correction for electron attachment was applied to the calibration pulses as described above, to make the corrected pulse height the same as that of a pulse produced by the same amount of ionization distributed generally.

6. EXPERIMENTAL RESULTS

Table I gives the results of experiment A. The column $n(J)$ is the number of events, with a pulse shape indicating general ionization, within the ionization limits listed in column 1 in the time t . J is expressed in units of 2.00×10^5 ion pairs, the ionization produced by a calibration α -particle. $N(J)$ is the number of events per hour with an ionization greater than the lower of the corresponding limits in column 1, and ΔN is approximately the statistical uncertainty $N^{1/2}/t$. Actually, it is somewhat larger than this because air-shower tray information was not available for all pulses and the application of a correction for air showers to that part of the burst rate for which air-shower bursts could not be directly eliminated increased the probable error slightly.

The number of events with a pulse shape indicating more or less local ionization was 0.13 per hour with a pulse size greater than $1.5 h_\alpha$. The corresponding frequencies of pulses of size greater than 2.0, 3.0, and $4.0 h_\alpha$ were 0.05, 0.02, and 0.007 per hour, respectively.

The results of experiment B, both with and without the additional 6 inches of lead between the coincidence tray and the top of the pile, are presented in Table II in a similar manner.

7. THEORETICAL BURST-SIZE-FREQUENCY DISTRIBUTIONS

a. General Considerations

The differential energy spectrum gives the number of μ -mesons between the energies E_0 and E_0+dE_0 in a

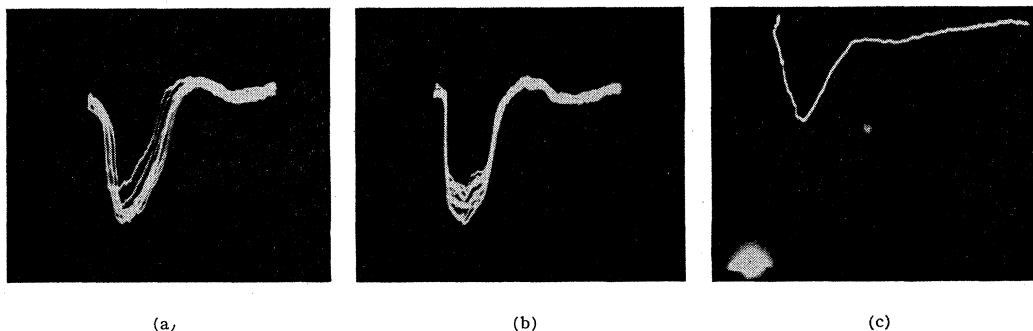


FIG. 6. Photographs of synchroscope traces. (a) A group of α -particle pulses produced by a source 4 inches from the collecting wire. (b) Same as (a) with $r=1$ inch. (c) Cosmic-ray burst pulse involving 4.0×10^6 ion pairs. The light in the lower left corner indicates a coincidence with the air-shower tray.

TABLE I. Burst rates, experiment A.

J ionization units	$n(J)$ events	t hours	$N(J)$ per hour	ΔN per hour
1.2-1.49	514	447	3.54	0.08
1.5-1.99	539	589	2.38	0.07
2.0-2.49	311	611	1.49	0.05
2.5-2.99	171	611	0.985	0.044
3.0-3.99	208	611	0.707	0.039
4.0-4.99	95	611	0.366	0.031
5.0-5.99	48	611	0.211	0.026
6.0-	81	611	0.132	0.022

differential solid angle, $\sin\theta d\theta d\phi$. If this is multiplied by the probability $\sigma_i(E_0, \epsilon) d\epsilon dx$ of an interaction in a thickness of material, dx , resulting in the production of a soft secondary (knock-on electron or bremsstrahlung photon) of energy ϵE_0 and by the probability $P(\epsilon E_0, x, S)$ of a shower with a number of particles greater than S resulting from this secondary after traversing a thickness x of material, a differential expression is obtained for the number of bursts of this or greater size hitting the chamber. The ionization produced in the chamber by such a burst is related to the burst size by the average path length in the chamber of the electrons in the burst. If the expression resulting from this relation is integrated or summed over the variables θ , ϕ , x , ϵ , and E_0 , and over the variables describing the position at which the shower hit the chamber, the number of events is obtained in which an ionization greater than a given amount is produced in the chamber.

As will be shown, the μ -meson spectrum at sea level is of the form

$$n(E_0, \theta) = ce^{-\alpha E_0} / (E_0 + k \sec\theta)^m.$$

The functions of θ and ϕ introduced by a consideration of the present geometry would make it necessary to integrate the integral over θ numerically and, consequently, the subsequent integrals over ϵ and E_0 would become prohibitively lengthy. It is more convenient to separate the integration over θ from the integrations over ϵ and E_0 by dividing the upper hemisphere into regions which will be specified by an index G , such that the denominator in the above expression does not change significantly within a particular region. This gives rise to a series of spectra,

$$n_G(E_0) dE_0 d\Omega = ce^{-\alpha E_0} dE_0 d\Omega / (E_0 + k_G)^m,$$

where $k_G = k(\sec\theta)_G$ and $\theta_{G \min} \leq \theta < \theta_{G \max}$.

The number of bursts with more than S electrons per square meter per hour per unit solid angle, $N_{iG}(S)$, arising from process i in region G may then be found by integrating $P(\epsilon E_0, S)$ over all possible ϵE_0 weighted by the appropriate number of secondaries of energy ϵE_0 . This is expressed by the following integral:

$$N_{iG}(S) d\Omega = d\Omega \int_0^\infty dE_0 n_G(E_0) \int_0^{\epsilon_m} d\epsilon \sigma_i(E_0, \epsilon) P(\epsilon E_0, S).$$

TABLE II. Burst rates, experiment B.

J ionization units	Without lead 312 hours		With lead 308 hours	
	$N(J)$ per hour	ΔN per hour	$N(J)$ per hour	ΔN per hour
1.5	0.450	0.038	0.315	0.032
2.0	0.240	0.028	0.169	0.024
2.5	0.148	0.022	0.103	0.018
3.0	0.099	0.018	0.070	0.015
4.0	0.053	0.013	0.039	0.010
5.0	0.032	0.010	0.023	0.009

The voltage pulse produced by a burst, which is proportional to the number of ion pairs J depends not only on S but also on the path length in the chamber of these S particles. If q is the number of ion pairs produced per unit path length by an electron of an energy equal to the average energy of electrons in a burst and \bar{p} is the average path length of the electrons in the burst, then $J = q\bar{p}S$.

It is thus necessary to determine the differential spectrum of path lengths in the chamber in each of the regions G . This is most conveniently accomplished by determining the integral path spectrum and performing a numerical differentiation. The quantity $A(p, \theta, \phi)$, which is the area of the chamber over which a particle entering the chamber from the solid angle $d\Omega$ around (θ, ϕ) has a path length $\geq p$, will be integrated over $0 \leq \phi \leq 2\pi$ and $\theta_{G \min} \leq \theta \leq \theta_{G \max}$, giving the total aperture of the chamber for a path length $\geq p$ in region G ,

$$A_G(p) = 4 \int_{\theta_{G \min}}^{\theta_{G \max}} d\theta \sin\theta \int_0^{\pi/2} d\phi A(p, \theta, \phi).$$

$A_G(p)$ is then numerically differentiated to give $a_G(p) dp$, the aperture of the chamber in region G for path lengths between p and $p+dp$. If one particle were incident at random per unit area per unit time from region G , $a_G(p)$ would be the number per unit time which hit the chamber and had a subsequent path length in the chamber between p and $p+dp$.

The number of bursts $N_G(J)$ which produce an ionization in the chamber $> J$ is

$$N_{iG}(J) = \int_0^\infty dp a_G(p) N_{iG}\left(\frac{J}{q\bar{p}}\right);$$

that is, it is the number of bursts for which $q\bar{p}S > J$. In the final evaluation, this integral will be replaced by a summation over the apertures, $a_G(p) \Delta p$.

Finally, we sum $N_{iG}(J)$ over the subscripts i and G to obtain the total-ionization-frequency distribution $N(J)$ for the chamber:

$$N(J) = \sum_i \sum_G N_{iG}(J).$$

b. The μ -Meson Energy Spectrum

In the absence of any accurate direct determinations, the best estimate of the vertical μ -meson energy spec-

trum at sea level is obtained by transforming a depth-intensity relationship for cosmic rays (the measurements of Wilson¹¹ will be used) into an energy-intensity relationship using a range-energy correlation. Cosmic rays far underground consist of μ -mesons and associated soft secondaries. Randall's¹² estimate of the number of such soft secondaries included in Wilson's counting rates will be used to correct these underground data. This method is valid up to energies of the order of 2×10^{11} ev. Beyond this point, certain processes of a catastrophic nature become important (precisely those processes which result in the bursts under investigation).

Lyons¹³ has investigated the effect of these catastrophic events and finds that they result in an exponential decrease superimposed on the power law in the depth spectrum. Wilson's data may be rather well represented by the analytical expression $N(h) \sim h^{-\gamma'} e^{-\alpha' h}$, where N is the frequency of mesons observed at a depth h in meters of water equivalent, and $\alpha' = 1/(2000 \text{ m.w.e.})$. It has been pointed out^{14,15} that the knock-on and bremsstrahlung cross sections for spin $\frac{1}{2}$ μ -mesons are too small by about a factor of 10 to account for this observed value of α' and that the deviation results from a deviation in the μ -meson energy spectrum at sea level which may be explained on the basis of the competition between nuclear interactions and decay for π -mesons in the atmosphere.

The vertical differential μ -meson energy spectrum obtained from this transformation is

$$n(E_0, 0) dE_0 d\Omega = C e^{-\alpha E_0} d\Omega dE_0 / (E_0 + 1.8 \times 10^9)^\gamma,$$

with $\alpha = 1/(5 \times 10^{11} \text{ ev})$ and $\gamma = 2.9$ for $E < 10^{11}$ ev and $\gamma = 3.1$ for $E > 10^{11}$ ev. 1.8×10^9 ev is the energy required for a μ -meson to reach sea level from an average point of production. C was taken to be $0.160 \times 10^{17.1}$ in order to normalize the integrated spectrum to Greisen's¹⁶ experimental value at sea level.

The effect of increasing θ on this energy distribution is to increase the path length and thus the energy loss in reaching sea level. Since the relationship between range and energy is essentially linear for energies of the order of 1.8×10^9 ev, where only ionization is important, we finally have

$$n(E_0, \theta) dE_0 d\Omega = C e^{-\alpha E_0} d\Omega dE_0 / (E_0 + 1.8 \times 10^9 \sec \theta)^\gamma.$$

c. The Shower Function, $P(\epsilon E_0, S)$

$P(\epsilon E_0, x, S)$ was defined as the probability of occurrence of a shower containing more than S particles at a distance x from the position of a μ -meson interaction in which an energy ϵE_0 was transferred to a soft

secondary. The function,

$$P(\epsilon E_0, S) = \int_0^\infty P(\epsilon E_0, x, S) dx,$$

is roughly a measure of the distance over which a shower of energy ϵE_0 contains more than S particles. This function depends not only on the average behavior of cascade showers, which is rather well known, but also upon the form and magnitude of the fluctuations in S from shower to shower, a subject which, at present, is in a considerably more unsettled state.

Christy and Kusaka³ proposed an analytical approximation for the average behavior of a shower in the vicinity of the maximum of the shower development which agrees well with the recent calculations of Bernstein.¹⁷ However, their expression for the average behavior was derived by considering only the longitudinal development of the shower, an approximation which is also used by Bernstein and which is valid for the high energy electrons in a shower but which breaks down completely for the lowest energies involved.

Roberg and Nordheim¹⁸ have investigated the lateral development of cascade showers. They have calculated the fraction of electrons in a shower which have a root-mean-square scattering angle of one radian or more. This fraction, which to some extent measures the degree of failure of the longitudinal approximation, is one-sixth for material of low atomic number and increases to about four-fifths for lead. Wilson¹⁹ has investigated the effect of scattering on the longitudinal development of a shower using a Monte Carlo method for lead and finds a reduction in the number of electrons at depths near the maximum of shower development by a factor of two compared to the results obtained neglecting scattering. We might expect a corresponding reduction in brick of the order of 15 or 20 percent. The effect of this reduction on the amount of ionization observed in an ion chamber is dependent on the chamber geometry and may result in a considerably smaller change in the ionization. Considerations of chamber geometry indicate that 95 percent of the bursts observed in the present experiment A have path lengths of less than 0.5 meter and that, for most of these, the effect of angular deviations from the shower is to increase the average path length in the chamber of the electrons in the burst as compared to the axis length. This increase in ionization compensates to some extent for the loss of electrons resulting from scattering.

Since the burst rate is a rapidly decreasing function of burst energy, the effect of fluctuations is to increase the burst rate. Christy and Kusaka³ showed that the burst rate using the Furry expression for fluctuations was 2.2 times the burst rate R_0 which would be predicted on the basis of no fluctuations. Using the value

¹¹ V. C. Wilson, Phys. Rev. **53**, 377 (1938).

¹² C. A. Randall, unpublished thesis, University of Michigan (1950).

¹³ D. Lyons, Physik. Z. **42**, 166 (1941).

¹⁴ K. I. Greisen, Phys. Rev. **73**, 521 (1948).

¹⁵ S. Hayakawa, Prog. Theoret. Phys. **3**, 199 (1948).

¹⁶ K. I. Greisen, Phys. Rev. **61**, 212 (1942).

¹⁷ I. B. Bernstein, Phys. Rev. **80**, 995 (1950).

¹⁸ J. Roberg and L. W. Nordheim, Phys. Rev. **75**, 444 (1949).

¹⁹ R. R. Wilson, Phys. Rev. **79**, 204 (1950).

obtained by Nordsieck, Lamb, and Uhlenbeck²⁰ for the second moment of the S distribution, $\sigma = \frac{1}{2}\bar{S}^2$ as compared to $\sigma = \bar{S}^2$ for the Furry model, they estimated a burst rate of $1.55R_0$. However, Scott and Uhlenbeck²¹ recalculated this second moment and found a considerably lower value which, on the basis of one numerical calculation for the case of their cosmic-ray shower model is of the order of $\sigma = 3\bar{S}$. It is estimated that the burst rate obtained using this figure, taking into account the reduced asymmetry of the distribution as compared to the Furry distribution, is $1.3R_0$. This figure, which is somewhat energy dependent, applies to the average energy involved in the present observations and should not be in error by more than 10 percent. An accurate calculation rather than an estimation is not in order since the information available on the fluctuations themselves is so meager.

d. Cross Sections for Spin $\frac{1}{2}$ μ -Mesons

The cross section for bremsstrahlung was derived by Heitler.⁴ If his nomenclature is modified by letting $\epsilon = k/E_0$ and $E = E_0 - k$, and if the radius of the nucleus is introduced as the lower limit to his integration over the impact parameter, the cross section is

$$\sigma(E_0, \epsilon)d\epsilon = \frac{16}{3}d\epsilon \left[\frac{3\epsilon}{4} + \frac{1-\epsilon}{\epsilon} \right] \left[\ln \frac{12E_0(1-\epsilon)}{5\mu c^2 \epsilon} - \frac{1}{2} \right],$$

where σ is measured in units of $(e^2/\mu c^2)^2 \alpha Z^2$. Screening of the Coulomb field of the nucleus by the atomic electrons causes this cross section to become essentially independent of E_0 above an energy such that $(E_0/\mu^2 c^2) \sim \hbar/mc^2 Z^{\frac{1}{2}}$ or $E_0 \sim 9 \times 10^{11}$ ev for aluminum.

For the knock-on process, Bhabha²² has derived a cross section which, for the case of $E_0 \gg \mu c^2$, reduces to

$$\sigma(E_0, \epsilon)d\epsilon = \frac{2\pi e^4}{mc^2} \frac{1}{E_0} \frac{d\epsilon}{\epsilon^2} \left[1 - \frac{\epsilon}{\epsilon_m} + \frac{\epsilon^2}{2} \right]$$

per electron. $\epsilon_m = [1 + (\mu^2 c^2 / 2mE_0)]^{-1}$ for large E_0 , where ϵ_m is the maximum fractional energy transferable by a meson (energy E_0 , mass μ) to an electron (mass m).

Bhabha^{23,24} has derived a cross section for the direct production of an electron-positron pair by a relativistic particle of mass M in the field of a nucleus of charge Z . If we let $E = E_- + E_+$, where E_- and E_+ are the individual energies of the pair, this cross section is

$$dQ(\gamma, E, E_-) = (8/\pi)(\alpha Z)^2 r_0^2 m^2 c^4 \gamma^2 E^{-4} \ln 2k\gamma dE dE_-,$$

which was derived under the condition that $mc^2\gamma \ll (E_-, E_+) \ll Mc^2\gamma$, where m is the electron rest mass,

$\gamma = 1/(1-v^2/c^2)^{\frac{1}{2}}$ for the incoming particle, and k is an indeterminant factor of the order of unity.

Integrating over E_- from $\gamma c^2 m$ to $\gamma c^2 (M-m)$, we obtain the total cross section for the production of a pair with energy between E and $E+dE$,

$$Q(\gamma, E)dE = (8/\pi)(\alpha Z)^2 r_0^2 m^2 c^4 \gamma^2 E^{-4} (E - 2\gamma mc^2) \ln 2k\gamma dE.$$

Screening becomes important when $E \lesssim 2\gamma^2 mc^2 / 183Z^{-\frac{1}{2}}$. For these small energies, $\ln 2k\gamma \rightarrow \ln 183Z^{-\frac{1}{2}} kE/\gamma mc^2$. This integrated cross section is only an approximation, since the limits of integration violated the conditions of derivation. This is not important since, as will be shown, the contribution of this process to the production of large bursts is negligible.

e. The Calculations

The function $N_{iG}(S)$ is obtained by inserting the functions $P(\epsilon E_0, S)$, $\sigma_i(E_0, \epsilon)$, and $n_G(E_0)$ in the symbolic expression for $N_{iG}(S)$ given previously and by evaluating the integral over ϵ exactly and that over E_0 graphically. This was done for each region G and for $S=35, 180$, and 800 electrons using the cross sections for the bremsstrahlung and knock-on processes.

Relative to bremsstrahlung, the largest contribution to the burst distribution by pair production will be for small shower energies and thus for small S , since $Q_{\text{pair}} \sim E^{-3}$ and $\sigma_{\text{brem}} \sim E^{-1}$ for large E , where E is the shower energy. Evaluating $N_{pp,G}$ (35) by inserting $Q(\gamma, E)dE$ into a differential expression for $N_{iG}(S)$ and integrating over E from 0 to E_0 and over E_0 from 0 to ∞ gives a figure, $N_{pp,G}(35) = 0.06 \text{ m}^{-2} \text{ sterad}^{-1} \text{ hour}^{-1}$ independently of the region G , as compared to $N_{ko,G}(35) + N_{\text{brem},G}(35) = 2.55 \text{ m}^{-2} \text{ sterad}^{-1} \text{ hour}^{-1}$ for $G=I$. The pair production contribution will be relatively less for larger values of S and will be neglected.

$N_G(S) = \sum_i N_{iG}(S)$ is plotted in Fig. 7 for the regions $G=I, V$, and VII , the regions being defined by the following θ -limits: I (0° - 50°), II (50° - 63.4°), III (63.4° - 70°), IV (70° - 75°), V (75° - 80°), VI (80° - 83°), VIII (83° - 84.8°), and VIII (84.8° - 90°).

To obtain the number of events causing an ionization greater than $J = \bar{p}qS$, the summation $N(J) = \sum_G \sum_p a_G \times (\bar{p})NJ/\bar{p}q$ is performed, where N_G is obtained from Fig. 7, q is evaluated in Appendix I, and $a_G(\bar{p})$ is discussed in Appendix II. $N(J)$ was evaluated for $J=2 \times 10^5, 6 \times 10^5$, and 1.8×10^6 ion pairs and is plotted in Fig. 8 in comparison with the experimental points.

A fairly accurate estimate of the curve for spin 0 corresponding to that for spin $\frac{1}{2}$ in Fig. 8 may be obtained from the tabulated values of burst frequencies in Christy and Kusaka, interpreting their data for the present material rather than for lead. Table III gives the value of $N(S)$ for the bremsstrahlung and knock-on processes together. Corrections have been made for a ratio of meson-to-electron mass of 210 rather than 177 and for the Z dependence of the knock-on contribution.

The major contributions to $N(J)$ for $J=2 \times 10^5, 6 \times 10^5$, and 1.8×10^6 ion pairs come from bursts in the

²⁰ Nordsieck, Lamb, and Uhlenbeck, *Physica* 4, 344 (1940).

²¹ W. T. Scott and G. E. Uhlenbeck, *Phys. Rev.* 62, 497 (1942). The author is indebted to Professor Uhlenbeck for calling his attention to this recalculation.

²² H. J. Bhabha, *Proc. Roy. Soc. (London)* A164, 257 (1938).

²³ H. J. Bhabha, *Proc. Cambridge Phil. Soc.* 31, 394 (1935).

²⁴ H. J. Bhabha, *Proc. Roy. Soc. (London)* A152, 257 (1935).

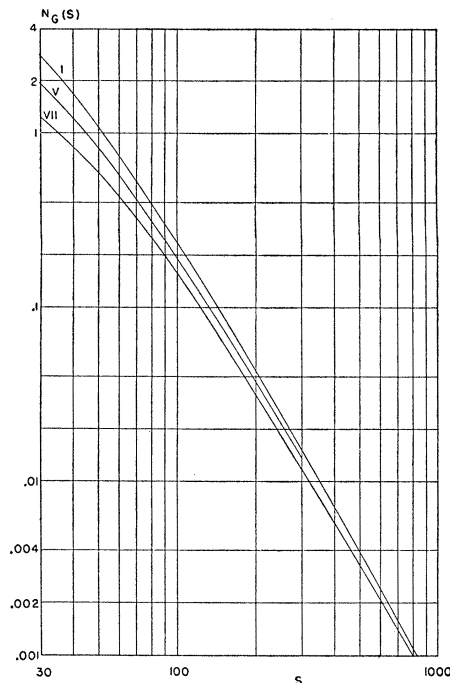


FIG. 7. The integral burst rate $N_G(S)$ per square meter per steradian in brick as a function of the number of particles S in the burst, for $G=I$ (top curve), $G=V$ (middle curve), and $G=VII$. The values for $G=II, III, \text{ and } IV$ lie between the top and middle curves while the values for $G=VI$ lie between the middle and bottom curves.

range $S=40-80$, $80-200$, and $160-600$, respectively. The ratio of $N(J)$ for spin 0 over that for spin $\frac{1}{2}$ will accordingly be taken as 0.65, 0.62, and 0.60, respectively, for these three values of J . These ratios are then used to plot the spin-0 curve in Fig. 8 relative to the curve for spin $\frac{1}{2}$.

8. DISCUSSION OF RESULTS

The uncertainties in the determination of the burst frequencies are not significantly greater than the statistical error $N^{1/2}/l$. The elimination of air showers, which amounts to a 3 percent correction for small bursts and to about 10 percent for large bursts, probably represents an overcorrection. Some of the eliminated bursts probably were caused by mesons associated with air showers, others being caused by similarly associated N component. The pulse sizes with which these frequencies are associated are uncertain by about 3 percent, which is equivalent to 6 percent in the frequency. The assumption concerning the equality in energy loss per ion pair for electrons and α -particles may be in error by 4 percent.

The energy spectrum of μ -mesons was estimated to have a probable error of 5 percent at 2×10^{11} ev and about 50 percent at 10^{12} ev which implies a 5 percent error in the calculated rate for small bursts and 15 percent for the largest bursts. The errors in the effect

of fluctuations and of the average behavior of showers are both estimated to be about 10 percent.

The over-all probable error of the comparison between the experimental results and the calculations is thus about 18 percent for small bursts and increases to 23 percent for the largest bursts.

Assuming that the calculated μ -meson burst rate for experiment B is correct (the results to be derived are not very sensitive to the validity of this assumption), the ratio of the bursts observed in excess of this calculated rate with and without lead is 0.61 which corresponds to a mean free path of 340 g cm^{-2} . This mean free path is defined in terms of the observed burst production decrease and should be intermediate between the two extreme cases of mean free path for complete absorption and for interaction. Fahy²⁵ has obtained a similarly defined mean free path of 346 g cm^{-2} in lead for the bursts observed at high altitudes which are about 98 percent nuclear interactions. The agreement, which is fortuitously good, makes it reasonable to attribute the bursts observed in excess of the calculated rate to the N component primaries responsible for nuclear interactions.

The burst rate in experiment A resulting from nuclear interactions may be calculated if an assumption is made concerning the angular distribution of the N component. The ratio of the number of bursts due to nuclear interaction to be expected in experiment A compared to that observed in experiment B, assuming a $\cos^2\theta$ distribution for the N component, is

$$\frac{\int A_G(\theta, \phi, \text{exp}A) \cos^2\theta d\Omega}{\int A_G(\theta, \phi, \text{exp}B) \cos^2\theta d\Omega} = 2.56.$$

The absolute rate of bursts in excess of that calculated for experiment B has been multiplied by this figure and subtracted from the rate observed in experiment A to give the corrected points in Fig. 8.

It should be noted that this result is not inconsistent with the results of the attempt to identify nuclear interactions by their pulse shape, which resulted in a negligible rate, since the triggering requirements are such as to almost completely eliminate the recording of events which produce an ionization of an entirely

TABLE III. Comparison of burst frequencies.

S	$N(S)$ (0)	$N(S)$ ($\frac{1}{2}$)	$N(0)/N$ ($\frac{1}{2}$)
20	5.7×10^{-7}	7.8×10^{-7}	0.73
40	1.35×10^{-7}	1.98×10^{-7}	0.68
80	3.0×10^{-8}	4.8×10^{-8}	0.63
160	6.5×10^{-9}	10.5×10^{-9}	0.62
320	1.31×10^{-9}	2.28×10^{-9}	0.58
640	2.5×10^{-10}	4.3×10^{-10}	0.58

²⁵ Edward F. Fahy, Phys. Rev. **83**, 413 (1951).

local character. The triggering probability is only increased by the presence of particles capable of penetrating the 1-inch Duralumin plate and recording on the bottom tray of Geiger tubes, and as this number increases, the discrimination according to pulse shape becomes more uncertain. It is also to be expected that a considerable fraction, if not the majority, of the recorded nuclear interaction bursts are produced by the soft showers initiated by the decay of π^0 mesons.

9. CONCLUSIONS

Lapp²⁶ has obtained burst data under 35 cm of iron using the Carnegie chamber for which Christie and Kusaka made their calculations. If we modify these calculations to the extent of changing the μ -meson mass to 210, renormalizing the μ -meson energy spectrum to the value used here and using 25.9 Mev for the critical energy in iron, we obtain a μ -meson burst rate, $N(S) = 8.3 \times 10^{-9} \text{ cm}^{-2} \text{ sec}^{-1} \text{ sterad}^{-1}$ for $S = 300$ particles as compared to the value observed by Lapp of 12.9×10^{-9} . Bremsstrahlung accounts for 80 percent of the calculated rate and knock-on for the remainder. The bursts observed by Lapp in excess of the calculated rate, which amount to 55 percent of the μ -meson rate, may be translated into an expected excess for the present experiment A by assuming that the nuclear interaction bursts arise primarily from π^0 decay and that the N component is absorbed exponentially. It will be further assumed that the transparency of the nucleus is independent of Z for the types of interactions involved. The mean free paths in iron and brick corresponding to 340 g cm^{-2} in lead are, respectively, 225 g cm^{-2} and 175 g cm^{-2} . The cross section for knock-on, bremsstrahlung, and nuclear interactions will each have a different Z dependence, but the material dependence of the subsequent shower development will be the same in each case. Using a Z^{+1} , Z^{+2} , and Z^{+3} dependence for knock-on, bremsstrahlung, and nuclear interactions, and correcting for the additional 0.94 mean free path of absorber in the present experiment, Lapp's data indicate a ratio of nuclear interactions to μ -meson bursts of 0.47 which agrees very well with the values observed in experiment A for large bursts of 0.43. The assumed Z dependences are consistent with the results of this comparison although they are not thereby individually verified.

Although the agreement between the corrected results and the calculations for spin $\frac{1}{2}$ μ -mesons is well within the probable error, this does not constitute conclusive evidence that the spin of the μ -meson is $\frac{1}{2}$, since it is not at present possible to evaluate the contribution to the burst rate of possible specifically nuclear interactions of the spin 0 μ -meson. However, the present data might be used, given independent evidence concerning both the spin of the μ -meson and the magnitude of its nuclear interactions, to obtain an ex-

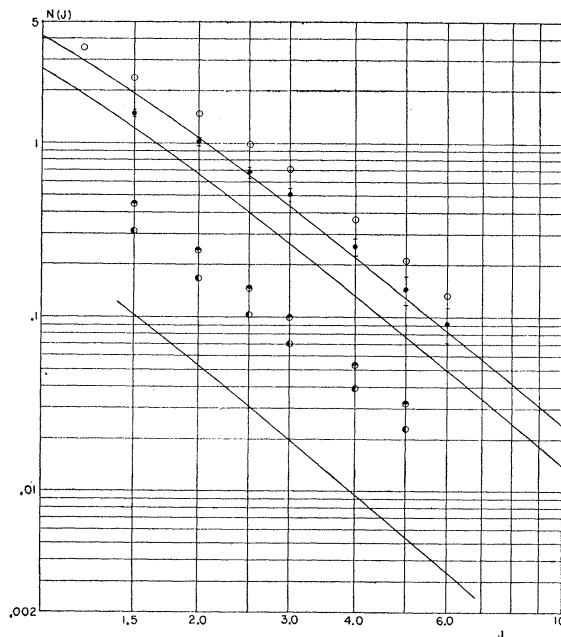


FIG. 8. The integral burst size-frequency distributions, $N(J)$, in bursts per hour for the present chamber and environment as a function of the number of ion pairs produced, J , in units of 2.00×10^6 ion pairs. The top and middle curves represent the calculated values for spin $\frac{1}{2}$ and spin 0 μ -mesons, respectively, in experiment A. The bottom curve is the calculated distribution for spin $\frac{1}{2}$ in experiment B. The experimental values are represented by the circles; (o) observed values in experiment A; (●) observed values in experiment B without the lead block; (◐) values in experiment B with the lead block; (◑) values in experiment A corrected for the estimated rate of nuclear interactions. The flags on these latter points represent the probable errors of the measurements.

perimental estimate of the electromagnetic cross sections.

The author is deeply indebted to Professor Wayne E. Hazen for his constant encouragement and advice during the course of this work. He is grateful to Mr. William P. Davis, Jr., for performing the tedious numerical integrations involved in evaluating the functions, $N_G(S)$, presented in Fig. 7.

APPENDIX 1

No reliable direct measurements of the average number of ion pairs produced by an electron per unit path length are available. This number (which is of course energy-dependent) may be estimated with some degree of accuracy, however, from the theoretical collision energy loss of an electron and from measurements of the average energy loss per ion pair produced.

It is not actually necessary to consider the total ionization produced by a burst in order to make comparisons with the theoretical predictions. We are interested essentially in the total energy expended in the chamber by a burst, and this may be derived directly from a comparison with the energy expended by a calibration α -particle if we know the ratio of the energy expended per ion pair formed by an α -particle (W_α) and by a high energy electron (W_β) in argon. Unfortunately, no measurements of these W are available using identical equipment and conditions, under which circumstance the effect of systematic errors in the measurements would tend to be negligible.

²⁶ R. E. Lapp, Phys. Rev. **69**, 312 (1946).

Curran, Cockroft, and Insch²⁷ have measured W_β with a proportional counter for electron energies of a few kev in various mixtures of argon and methane and arrive at an asymptotic value for low methane content of $W_\beta=28.5$ ev. However, they state without further explanation that there are indications that W_β for very pure argon could differ appreciably from this value. They also quote a private communication from Nicodemus giving a value of $W_\beta=26.9$ ev (experimental conditions, including gas purity, unknown).

Stetter²⁸ used an ionization chamber to measure W_α averaged over the complete path of a polonium α -particle in relatively pure argon and obtained a value of $W_\alpha=28.4$ ev. Schmieder²⁹ found a value of $W_\alpha=24.4$ ev under conditions which were, apparently, not fundamentally dissimilar.

A careful study of W for 340 Mev protons was made by Bakker and Segrè³⁰ and resulted in a figure for W_p of "a few percent" higher than 25.5 ev.

In view of the differences in experimental conditions and of the possible variations in systematic errors resulting from these differences, it is felt that these data are not inconsistent with the assumption that W is independent of the nature of the ionizing particle and, furthermore, that W is no more than slightly dependent on the energy of the ionizing particle. There is evidence³¹ that W_β increases significantly for energies of the order of a few hundred ev compared to the value for high energy but it appears to be essentially constant for energies greater than a few kev. It will accordingly be assumed that $W_\alpha=W_\beta=26.4$ ev.

Although the ion production occurs in argon, the energy distribution of the electrons in the burst is characteristic of the brick-duralumin combination since the amount of argon traversed is insufficient to produce an appreciable transition effect. Thus, the average energy near the maximum of the shower development is approximately the critical energy, that is, about 54 Mev. The Bloch⁹ formula for energy loss by ionization gives the energy lost in collisions involving energy transfers up to some maximum value W_m ,

$$-\frac{dE}{dx} = 2\pi\sigma Z r_0^2 \frac{mc^2}{\beta^2} \left[\ln \left(\frac{mc^2 \beta^2 W_m}{(1-\beta^2) I^2} \right) + (1-\beta^2) \right],$$

where σZ is the electron density in the material; r_0 is the classical radius of the electron $=e^2/mc^2$; β is the fractional velocity of the incident electron; and I is the average ionization potential of the traversed material.

Bloch has demonstrated that $I \sim I_0 Z$ for any substance where I_0 , if not quite constant, at least is a slowly varying function of Z . A value of I_0 of 11.5 rather than 13.5 will be used in accordance with the measurements of Wilson.¹⁰

In deciding what to use for W_m , the nature of the detection

²⁷ Curran, Cockroft, and Insch, *Phil. Mag.* **41**, 517 (1950).

²⁸ G. Stetter, *Z. Physik* **120**, 639 (1943).

²⁹ K. Schmieder, *Ann. phys.* **35**, 445 (1939).

³⁰ C. J. Bakker and E. Segrè, *Phys. Rev.* **81**, 489 (1951).

³¹ L. H. Gray, *Proc. Cambridge Phil. Soc.* **40**, 72 (1944).

process must be considered. The Bloch formula represents an integration of a cross section for production of a secondary electron of energy W times W itself. For events in which somewhat more than the minimum amount of energy needed to ionize an atom is transferred, the energy will, in general, show up in the ionization chamber as tertiary, etc., ion formation unless the range of the secondary is sufficient to cause it to leave the chamber; in that case, some of the ions will be produced in the duralumin plate and will not be collected. The logarithmic dependence of dE/dx on W_m makes it relatively insensitive to the choice of W_m . A value of 2×10^6 ev will be used, corresponding to a range of 20 cm in argon at the present pressure of 1.4 atmospheres. The figure of 20 cm represents a rough compromise between a value of 12 cm, which would be appropriate for the most frequent bursts, with a path length of the order of 24 cm in the chamber and the value of 75 cm, which should be used for the very much less frequent bursts with a path length of the order of 1.5 meter.

The energy loss to secondaries of energy less than 2×10^6 ev is found to be 3770 ev cm^{-1} . The ionization produced in the chamber by those secondaries whose energy is greater than this corresponds to an additional energy loss of 160 ev cm^{-1} . This figure is obtained by calculation the number of such secondaries and assuming that the energy lost by each is only 2×10^6 ev.

A polonium α -particle source has been used to calibrate the chamber. Since the polonium α -particle energy is 5.30 Mev, the maximum number of ion pairs, n_α , produced in the chamber by the calibration source is

$$n_\alpha = 5.30 \times 10^6 / 26.4 = 2.00 \times 10^5 \text{ pairs.}$$

The number of ion pairs produced per cm by electrons is

$$n_p = 3930 / 26.4 = 149 \text{ pairs cm}^{-1}.$$

APPENDIX 2

The sensitive volume of the chamber is a rectangular parallelepiped of length a , width b , and height c . The projected area of the chamber over which a particle traveling in the direction (θ, ϕ) will have a path length in the sensitive volume $\geq p$ may be shown to be $A(p, \theta, \phi) = ab \cos\theta + bc \sin\theta \cos\phi + ac \sin\theta \sin\phi - 2pa \sin\theta \times \cos\theta \sin\phi - 2pb \sin\theta \cos\theta \cos\phi - 2pc \sin^2\theta \sin\phi \cos\phi + 3p^2 \sin^2\theta \times \cos\theta \sin\phi \cos\phi$. This expression, multiplied by $\sin\theta$, is integrated to obtain the regional apertures $A_G(p)$. The integration limits for $p=0$ are from $0 \leq \phi \leq 2\pi$ and θ is restricted to the limits defining the region. In general, from any direction (θ, ϕ) , any p may be found from $p=0$ to $p=p_{\max}(\theta, \phi)$. It is necessary to restrict the limits of integration for $A_G(p)$, $p>0$, to those angles for which $p < p_{\max}(\theta, \phi)$. The limits of the ϕ integration will then be functions of p and θ and the limits of θ will be functions of p .

The functions $A_G(p)$ are differentiated numerically to give the differential apertures $a_G(p)$. It was shown that the effect on $a_G(p)$ of the angular divergence of the showers (the previous calculations assumed a one-dimensional shower development) was small, and corrections were applied.

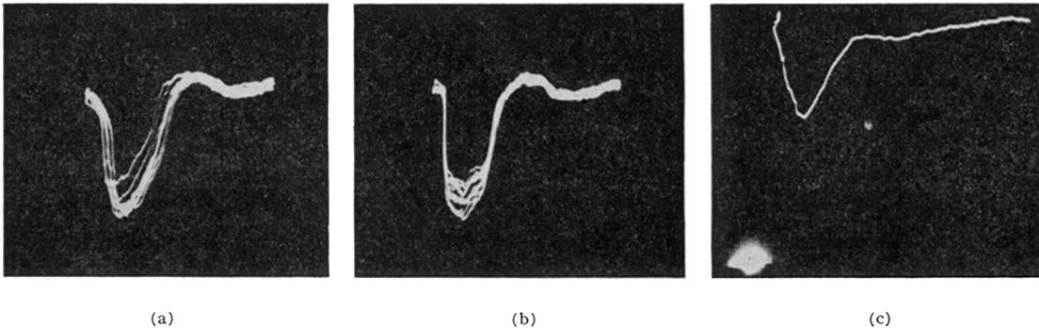


FIG. 6. Photographs of synchroscope traces. (a) A group of α -particle pulses produced by a source 4 inches from the collecting wire. (b) Same as (a) with $r = 1$ inch. (c) Cosmic-ray burst pulse involving 4.0×10^6 ion pairs. The light in the lower left corner indicates a coincidence with the air-shower tray.